MicroRNA-8063 targets heterogeneous nuclear ribonucleoprotein AB to inhibit the self-renewal of colorectal cancer stem cells via the Wnt/β-catenin pathway

ZHENG-QUAN CHEN[*], TAO YUAN[*], HANG JIANG[*], YUAN-YUAN YANG, LIN WANG, RUI-MIN FU, SHENG-QIANG LUO, TAO ZHANG, ZHEN-YU WU and KUN-MING WEN

Department of Gastrointestinal Surgery, Affiliated Hospital of Zunyi Medical University, Zunyi, Guizhou 563003, P.R. China

Abstract. The presence of cancer stem cells (CSCs) is a major cause of therapeutic failure in a variety of cancer types, including colorectal cancer (CRC). However, the underlying mechanisms that regulate the self-renewal of colorectal cancer stem cells (CRCSCs) remain unclear. Our previous study utilized CRCSCs and their parent cells; through gene microarray screening and bioinformatics analysis, we hypothesized that microRNA (miR)-8063 may bind to, and regulate the expression of, heterogeneous nuclear ribonucleoprotein AB (hnRNPAB) to facilitate the regulation of CRCSC self-renewal. The aim of the present study was to confirm this conjecture through relevant experiments. The results indicated that compared with that in parent cells, miR-8063 expression was significantly downregulated in CRCSCs, while hnRNPAB expression was increased. Furthermore, hnRNPAB was identified as a direct target of miR-8063 using a dual-Luciferase assay. Overexpression of hnRNPAB promoted the acquisition of CSC characteristics in CRC cells (increased colony formation ability, enhanced tumorigenicity, and upregulated expression of CSC markers), as well as the upregulation of key proteins (Wnt3a, Wnt5a and β-catenin) in the Wnt/β-catenin signaling pathway. Similarly, after silencing miR-8063 in CRC cells, the characteristics of CSC were altered, and the expression of hnRNPAB protein was promoted. However, post overexpression of miR-8063 in CRCSCs, the self-renewal ability of CSCs was weakened with the downregulation of hnRNPAB protein, Wnt3a, Wnt5a and β-catenin. These results suggest that as a tumor suppressor, miR-8063 is involved in regulating the self-renewal of CRCSCs, where loss of miR-8063 expression weakens its inhibition on hnRNPAB, which leads to the activation of Wnt/β-catenin signaling to promote the self-renewal of CRCSCs.

Introduction

Colorectal cancer (CRC) is a common malignancy of the digestive system, with incidence and mortality rates that rank third and second among all cancers worldwide, respectively (1). Surgical resection and chemoradiotherapy are the primary methods of CRC treatment. However, despite advancements in these modalities, the therapeutic effect on CRC is unsatisfactory, as the overall survival rate of patients remains at ~65% (2). Increasing evidence has verified the presence of cancer stem cells (CSCs) in tumor tissues, which are the origin of cancers and essential for metastasis, recurrence and drug resistance (3,4). CSCs have the potential for high tumorigenicity, self-renewal and unlimited proliferation, and exhibit the characteristics of normal cancer cells (5-7). Conventional chemoradiotherapy is effective against common cancer cells, but ineffective against CSCs; thus, targeting CSCs has the potential to eradicate cancer at the developmental stage (8-10). Although major advances have been made in the molecular characterization of CSCs, the molecular regulation of their tumor-initiation capacity is poorly understood. Therefore, it is imperative to further investigate the molecular mechanisms of CSCs to identify novel targets for CRC treatment.

Octamer-binding transcription factor 4-B1 (OCT4B1) is involved in regulating the self-renewal of colorectal cancer stem cells (CRCSCs), as was indicated in our previous study, in which four groups of cells with different OCT4B1 expression levels (different CSCs self-renewal ability) were established (11). This was later confirmed using an Affymetrix microarray, where the expression trend of heterogeneous nuclear ribonucleoprotein AB (hnRNPAB) was found to mirror that of OCT4B1, while opposing that of miR-8063. Furthermore, bioinformatics analysis indicated that miR-8063 and hnRNPAB may share common binding sites (11).

Correspondence to: Dr Kun-Ming Wen, Department of Gastrointestinal Surgery, The Affiliated Hospital of Zunyi Medical University, 149 Dalian Road, Huichuan, Zunyi, Guizhou 563003, P.R. China
E-mail: 381224619@qq.com

[*]Contributed equally

hnRNPAB belongs to the family of heterogeneous nuclear ribonucleoproteins (hnRNPs), a class of RNA-binding proteins that are closely associated with the biological functions of mRNAs. As such, hnRNPs are involved in nucleic acid metabolism, including RNA splicing, maintenance of telomerase activity, cell signal transduction, and regulation of transcription and translation (12-14). hnRNPAB (also known as hnRNPA/B) is divided into four subgroups: hnRNPA1, hnRNPA2/B1 (also known as hnRNPA2 or hnRNPB1), hnRNPA3 and hnRNPA0 (12,15). While hnRNPA1 and hnRNPA2/B1 have been widely studied, studies on hnRNPA0 and hnRNPA3 are limited. Notably, hnRNPAB and its subgroups are closely associated with malignant biological behaviors such as proliferation and apoptosis reduction, as well as poor patient prognosis in various cancer types (16-21). Our previous study confirmed the upregulation of hnRNPAB expression in CRC tissues compared with adjacent tissues, which was closely associated with poor prognosis (21). hnRNPAB and its subgroups were also found to regulate the epithelial-mesenchymal transition (EMT) of cancer cells, thus promoting metastasis (22-24). Increasing evidence also indicates that cancer cells can acquire CSC characteristics through EMT (25-27). Therefore, hnRNPAB may be involved in the regulation of CRCSCs.

Emerging evidence has indicated that hnRNPAB and its subgroups can regulate the expression of Wnt/β-catenin signaling pathway proteins. Stockley *et al* (28) discovered that the colony-formation ability of prostate cancer cells was decreased following hnRNPA2/B1-knockdown, while the proliferative ability was improved following overexpression of hnRNPA2/B1. These effects are related to the enhanced expression of β-catenin mRNA by hnRNPA2/B1, hence increasing the synthesis of β-catenin protein. Meng *et al* (29) revealed that hnRNPA1 promoted the differentiation of mesenchymal stem cells into cartilage cells, which is associated with enhanced expression of Wnt3a, Wnt5a and β-catenin. The Wnt/β-catenin signaling pathway is involved in the regulation of various CSC types, which has been confirmed by several studies (30-33). Therefore, hnRNPAB may regulate CRCSCs through the Wnt/β-catenin signaling pathway.

MicroRNAs (miRNAs/miRs) are a class of small non-coding single-stranded RNAs comprising ~18-25 nucleotides. miRNAs regulate post-transcriptional gene expression by binding to the 3' untranslated region (3'-UTR) of specific mRNAs, resulting in translational repression or mRNA degradation (34,35). Previous studies have suggested that miRNAs also play an important role in maintaining the self-renewal and drug resistance of CSCs (36-41).

In view of our previous studies and the associated literature, we hypothesize that miR-8063 may bind to hnRNPAB and regulate its expression, promoting Wnt/β-catenin signaling pathway activation to regulate the self-renewal of CRCSCs. Therefore, the purpose of the present study was to determine whether miR-8063 and hnRNPAB are involved in the regulation of CRCSC self-renewal, as well as the underlying molecular mechanisms involved.

Materials and methods

Cell lines and 3D microsphere culture. Human colorectal cancer cell lines (SW480 and HT29) and 293T cells were purchased from the Cell Bank of the Chinese Academy of Sciences (Shanghai, China). The cells were cultured in L-15 or DMEM medium (Hyclone; Cytiva) containing 10% fetal bovine serum (FBS) (Gibco; Thermo Fisher Scientific, Inc.). On reaching 80% confluency, SW480 and HT29 cells in the logarithmic growth phase were seeded into low-adhesion 12-well plates ($1x10^5$ cells/well) and maintained in stem cell culture medium: 25 μl B27 (1:50; Gibco; Thermo Fisher Scientific, Inc.), 20 μl EGF (20 ng/ml; Invitrogen; Thermo Fisher Scientific, Inc.), 15 μl basic fibroblast growth factor (bFGF; 10 ng/ml; Invitrogen; Thermo Fisher Scientific, Inc.) and 940 μl L-15 medium. The stem cell culture medium was replenished every 72 h, and the cells were cultured continuously for 14 days; the resulting SW480-3D and HT29-3D cell microspheres were maintained in stem cell culture medium and harvested for subsequent experimentation as required.

Patients and tissue samples. A total of 118 primary CRC and paired-adjacent tissue samples were collected from patients with CRC at the Affiliated Hospital of Zunyi Medical University (Zunyi, China), who underwent radical resection in a blinded manner between January 2015 and December 2015. The patient data are presented in Table I. CRC diagnosis was based on histopathological features. No patient underwent radiotherapy or chemotherapy preoperatively. Following surgery, the tissue samples were immediately stored at -80˚C for reverse transcription-quantitative (RT-q)PCR analysis. A 5-year follow-up survey of the patients was performed to determine their survival status. The present study was reviewed and approved by the Ethics Review Committee of the Affiliated Hospital of Zunyi Medical University (approval no. [2015] 1-040), and written informed consent was obtained from all patients.

RT-qPCR. Total RNA from tissues and cells was extracted using TRIzol® reagent according to the manufacturer's instructions (Takara Biotechnology Co., Ltd.), and reverse transcribed into cDNA using the Prime Script RT kit (Takara Biotechnology Co., Ltd.). Subsequent qPCR detection was performed using the 7500 Real-Time PCR System (Applied Biosystems; Thermo Fisher Scientific, Inc.) with a 20 μl reaction mixture comprising 10 μl qPCR SYBR Green Mix (Takara Biotechnology Co., Ltd.), 0.8 μl each of the forward and reverse primers, 2 μl cDNA and diethyl pyrocarbonate-treated H_2O up to the final volume. The qPCR conditions were: Initial denaturation at 95˚C for 30 sec, followed by 40 cycles of denaturation at 95˚C for 5 sec, annealing at 60˚C for 30 sec and melting curve analysis. Each test set included three duplicate wells, and the experiment was repeated three times. Relative gene expression was normalized to that of GAPDH or U6, and calculated using the $2^{-\Delta\Delta Cq}$ method (42). The primers were designed and synthesized by General Biosystems, Inc., the sequence of which are as follows: miR-8063 forward, 5'-TGCGGTCAA AATCAGGAGTCGGGG-3' and reverse, 5'-CCAGTGCAG GGTCCGAGGT-3'; U6 forward, 5'-GCTCGCTTCGGCAGC ACA-3' and reverse, 5'-AACGCTTCACGAATTTGCGTG-3'; hnRNPAB forward, 5'-AAGAAGTCTATCAGCAGCAGC AGTATG-3' and reverse, 5'-CTCCACCTCCACCACCAC CTC-3'; and GAPDH forward, 5'-ATGACATCAAGAAGG TGGTGAAGCAGG-3' and Reverse, 5'-GCGTCAAAGGTG GAGGAGTGGG-3'.

Table I. Association between miR-8063 expression and the clinicopathological characteristics of patients with colorectal cancer.

Clinicopathological characteristics	Category	cases (n=118)	Low (n=52)	High (n=66)	χ^2-value	P-value
			microRNA-8063 expression			
Age, years	<60	42	20	22	0.334	0.564
	≥60	76	32	44		
Sex	Male	65	28	37	0.058	0.810
	Female	53	24	29		
Tumor site	Rectum	89	41	48	0.587	0.443
	Colon	29	11	18		
Tumor infiltration	T1+T2	33	21	12	7.117	0.008
	T3+T4	85	31	54		
Vascular invasion	Negative	48	28	20	6.681	0.010
	Positive	70	24	46		
Differentiation status	High + moderate	34	18	16	1.526	0.217
	poor	84	34	50		
Lymph node metastasis	Negative	43	25	18	5.435	0.020
	Positive	75	27	48		
TNM stage	I+II	44	27	17	8.515	0.004
	III+IV	74	25	49		

Western blotting. Total cellular protein was extracted, and its concentration determined, using the Protein Extraction kit and the BCA protein concentration kit (both Beyotime Institute of Biotechnology), respectively. Protein samples (40 μg) were separated using 10% SDS-PAGE and transferred to a PVDF membrane. After blocking with 5% skim milk for 1 h at room temperature, the membrane was incubated overnight at 4˚C with anti-hnRNPAB (cat. no. 14813-1-AP; 1:2,000), anti-Wnt3a (cat. no. 26744-1-AP; 1:2,000), anti-Wnt5a (cat. no. 55184-1-AP; 1:2,000), anti-β-catenin (cat. no. 17565-1-AP; 1:2,000) and anti-β-tubulin (cat. no. 10094-1-AP; 1:5,000) (all ProteinTech Group, Inc.). The following day, the membrane was washed three times with PBS containing 0.1% Tween-20, and incubated with a horseradish peroxidase-conjugated antibody solution (cat. no. SA00001-2; 1:10,000; ProteinTech Group, Inc.) for 1 h at room temperature. Protein bands were visualized using Super ECL plus super-sensitive luminescent solution (Bio-Rad Laboratories, Inc.) and exposed using X-ray film. Quantity One software v4.6.6 (Bio-Rad Laboratories, Inc.) was used to quantify band intensities.

Dual-luciferase reporter assay. The target gene of hnRNPAB (miR-8063) was predicted using TargetScan (http://www.targetscan.org/vert_71/) bioinformatics software. The wild-type plasmid pmirGLO/hnRNPAB-3'UTR and the mutant plasmid pmirGLO/hnRNPAB-3'UTR-mut were constructed by General Biosystems, Inc. 293T cells (1x10^5/well) were seeded into 24-well plates 24 h before transfection. Cells were co-transfected with pmirGLO/hnRNPAB-3'UTR or pmirGLO/hnRNPAB-3'UTR-mut and miR-8063 mimics using Lipofectamine® 3000 (Invitrogen; Thermo Fisher Scientific, Inc.). After transfection for 48 h, the dual-luciferase reporter assay kit (Beyotime Institute of Biotechnology) was used according to the manufacturer's instructions, and the relative light unit (RLU) value was determined using the FLx800 fluorescence analyzer (BioTek Instruments, Inc.). The firefly RLU value was normalized to that of *Renilla* luciferase.

Colony formation assay. A soft agar colony-formation assay was used to evaluate the CSC characteristics of HT29-3D microspheres, and the self-renewal ability of CRCSCs (SW480CSCs and HT29CSCs) after miR-8063 overexpression. First, two different concentrations of soft agarose (0.6 and 1.2%) were prepared. The 3D microspheres and corresponding parent cells were digested into a single cell suspension using Accutase enzyme (PAN-Biotech) and 0.25% trypsin (Hyclone; Cytiva), respectively. The digested cells were then resuspended in a medium containing 10% FBS (1x10^3 cells/ml), and mixed with 1.2% agarose at a 1:1 ratio. Then, 3 ml of the mixture was added to each 6-cm-diameter glass dishes, and left to solidify to form the lower agar layer. Medium and 0.7% agarose were then mixed at a 1:1 ratio, and 0.5 ml cell suspension was added to the mix, which was then added atop the previously prepared 1.2% agarose to form the upper agar layer. Finally, the culture dishes were incubated at 37˚C for 2 weeks. The number of colonies in each plate was counted using a light microscope.

For parent cells (SW480 and HT29), a plate colony-formation assay was used to detect CSC characteristics after hnRNPAB overexpression. Cells were seeded into 6-well plates (1x10^3/well) in 1 ml medium containing 10% FBS, and cultured at 37˚C for 2 weeks. Next, 1 ml 4% paraformaldehyde was added as a fixative at room temperature for 15 min, and 1 ml Giemsa dye was then added for 15 min at room temperature. The number of colonies was manually counted using a light microscope (>50 cells are considered a clone). Colony-formation rate=number of clones/number of seeded cells x100%.

In vivo tumorigenicity. A total of 12 male specific pathogen-free-grade NOD/SCID mice (weight, 20-25 g; age, 6 weeks) and 44 male BALB/C nude mice (weight, 15-20 g; age, 6 weeks) were used in the experiment. All mice were housed at 25˚C, 50% humidity and in specific-pathogen-free conditions with a 12/12-h light/dark cycle. Sterile food and water were provided daily. NOD/SCID mice and nude mice were purchased from the Animal Experimental Center, Institute of Radiology Medicine, Chinese Academy of Medical Sciences (Tianjin, China). NOD/SCID mice were used to evaluate the tumorigenicity of HT29-3D microspheres *in vivo*. HT29-3D microspheres and HT29 cells were harvested and counted. Then, 1×10^7 cells were collected and resuspended in 1 ml medium; ~100 μl suspension (containing 1×10^6 cells) was subcutaneously injected into the left armpits of NOD/SCID mice (six mice in each group). Similarly, 5×10^6 SW480 and HT29 cells (overexpressing hnRNPAB), SW480CSCs and HT29CSCs cells (overexpressing the miR-8063), and the corresponding NC cells, were subcutaneously injected into the left armpits of the nude mice. When the tumors had reached a maximum diameter of 15 mm, the mice were anesthetized with an intraperitoneal injection of 1% Pentobarbital (50 mg/kg), and then sacrificed by cervical dislocation. Tumor volume was calculated using the following formula: Tumor volume = ½ (length x width^2) (43).

Flow cytometric analysis. The expression of CSC markers was detected using flow cytometry. Cells in the logarithmic growth phase were homogenized into a single cell suspension. Then, 1×10^6 cells were resuspended in 100 ml PBS containing 5% bovine serum albumin and 10 μl fluorophore-conjugated primary anti-CD44-PE (cat. no. PE-6506), anti-CD133-PE (cat. no. PE-62403) and the corresponding negative control antibodies (cat. no. PE-48642) (all ProteinTech Group, Inc.). The cells were mixed and incubated for 10 min in the dark at 4˚C. After centrifugation (500 x g, 5 min at room temperature), the cells were washed three times with PBS and resuspended in 200 μl PBS each. Finally, NovoExpress software 1.2.4 (Novocyte; ACEA Biosciences, Inc.) was used to detect the percentage of fluorescence-positive cells.

Cell infection. The lentiviruses overexpressing hnRNPAB (hnRNPAB-GFP-PURO), miR-8063-mimic-GFP-PURO and miR-8063-inhibitor-GFP-PURO were purchased from Hanbio Biotechnology Co., Ltd. The miR-8063-inhibitor-GFP-PURO lentiviral vector sequence was as follows: 5'-UUCGGGGCUGAGACUAAAACU-3'. Cells (1×10^5) were seeded into 12-well plates 24 h before infection. The virus was used to infect the cells according to the optimal MOI value obtained in the pre-experiment: Lentivirus hnRNPAB-GFP-PURO (MOI of 30 for both SW480 and HT29), miR-8063-mimic-GFP-PURO (MOI of 20 for SW480CSCs, and 30 for HT29CSCs), and miR-8063-inhibitor GFP-PURO (MOI 20 for both SW480 and HT29). Then, 8 mg/ml Polybrene (Hanheng Biological Technology Co., Ltd.) and enhanced infection solution (Shanghai GeneChem Co., Ltd.) were added at 37˚C for 12 h, and then replaced with fresh medium. After a further 72 h, the cells were collected, and the effect of gene overexpression or silencing was determined by RT-qPCR or western blotting.
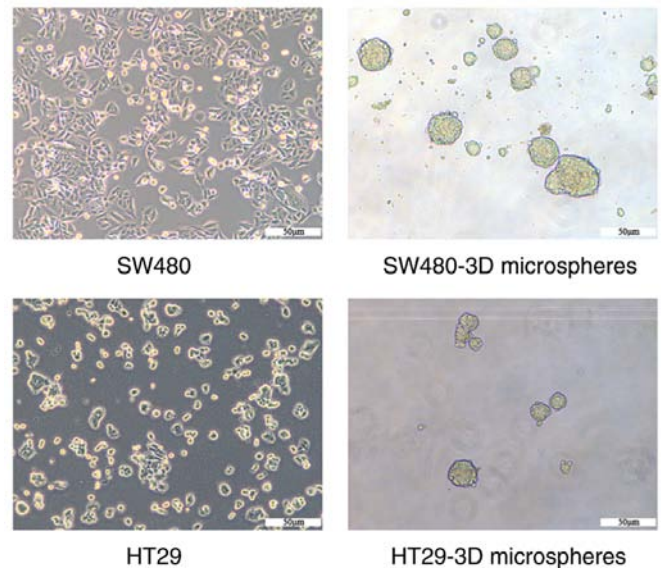

Figure 1. HT29-3D and SW480-3D parental cells and microspheres.

Statistical analysis. The data are expressed as the mean ± standard deviation. Multigroup comparisons were conducted by one-way ANOVA followed by Tukey's post hoc test. The χ^2 test was used to determine the association between miR-8063 expression and patient clinical characteristics. The Kaplan-Meier method was used to assess the association between overall survival rate and the expression level of miR-8063. P<0.05 was considered to indicate a statistically significant difference.

Results

SW480-3D and HT29-3D microspheres exhibit CSC properties. SW480-3D and HT29-3D microspheres were generated using a suspension culture of human CRC cells (SW480 and HT29; Fig. 1). A colony formation assay was performed to verify the self-renewal properties of the HT29-3D microspheres, and the results indicated that the colony-formation rates of HT29-3D microspheres and HT29 cells (45.67±9%) were significantly higher than those of the parent cells (16.98±5%) (Fig. 2A and B) (P<0.01). Next, the tumorigenicity of HT29-3D microspheres was detected using an *in vivo* tumorigenicity assay in NOD/SCID mice. The tumor volume of the mice inoculated with HT29-3D microspheres was significantly larger than that of the HT29 cell group, suggesting that HT29-3D microspheres had greater tumorigenicity than the parent cells (Fig. 2C and D) (P<0.01). Finally, the results of flow cytometry showed that the positive expression rates of CD44 in HT29-3D microspheres and HT29 cells were 37.14±1.62 and 9.37±2.28%, respectively. The corresponding positive expression rates of CD133 were 38.40±1.74 and 3.64±0.95%, respectively. These findings demonstrate significantly higher expression of CD44 and CD133 in HT29-3D microspheres compared with the parent cells (Fig. 2E and F) (P<0.01). The results suggest that HT29 microspheres exhibit CSC characteristics. SW480-3D microspheres with CSC characteristics were identified and
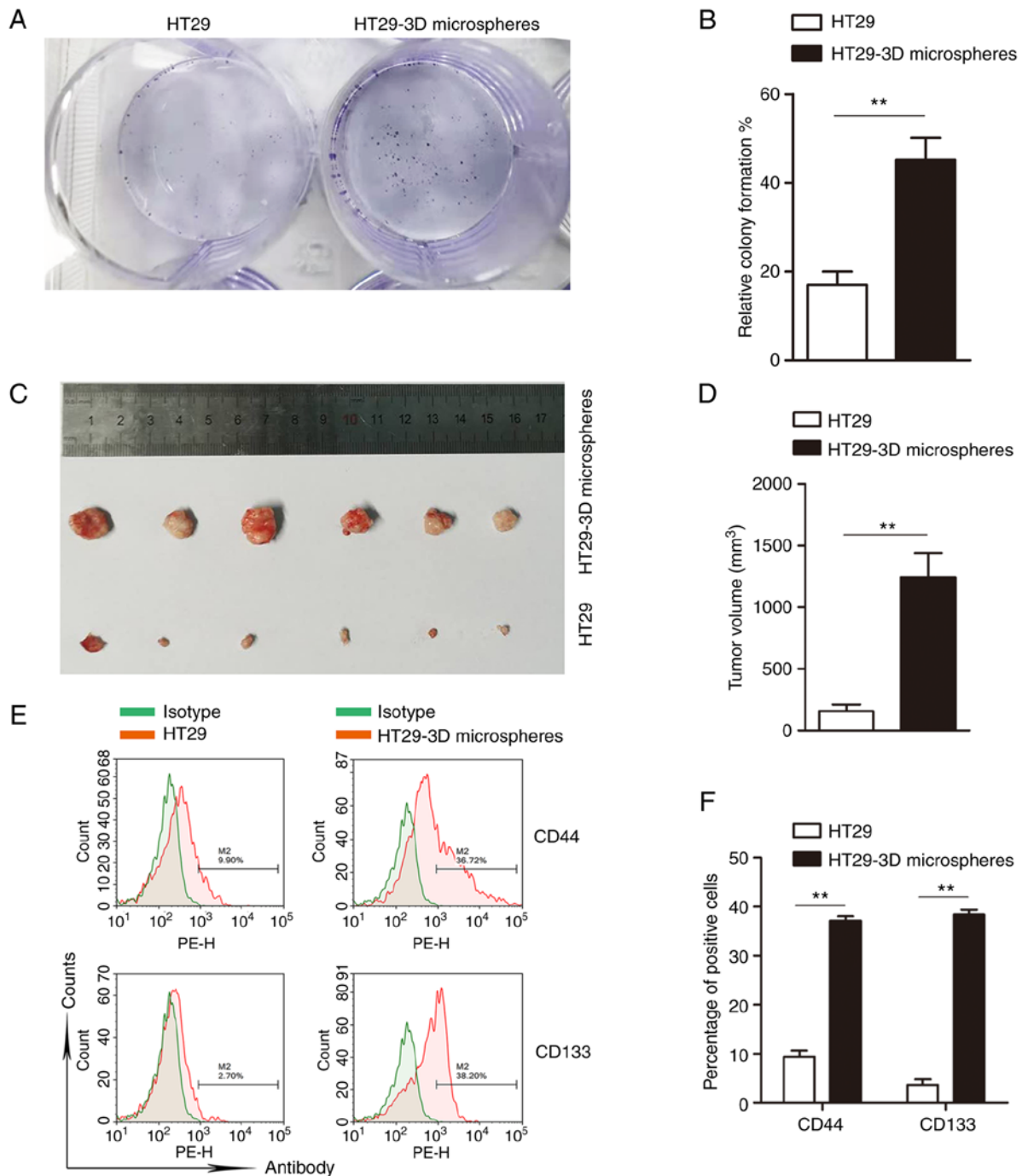
Figure 2. HT29-3D microspheres exhibit cancer stem cell properties. (A and B) Colony formation capacity of HT29-3D microspheres and parental cells. (C and D) Tumorigenic ability of HT29-3D microspheres *in vivo*, compared with that of HT29 parental cells. (E and F) Flow cytometric analysis revealed that HT29-3D microspheres were enriched for CD133^{+} and CD44^{+} cells, compared with the parental cell line. [**]P<0.01.

named SW480CSCs in our previous study (11). Similarly, HT29-3D microspheres were termed HT29CSCs.

miR-8063 expression is downregulated, while hnRNPAB expression is upregulated in SW480CSCs and HT29CSCs. RT-qPCR detection revealed that the relative expression levels of miR-8063 in SW480 and SW480CSCs were 1.03±0.04 and 0.45±0.06, respectively. miR-8063 expression in HT29 and HT29CSCs were 0.99±0.11 and 0.32±0.12, respectively (Fig. 3A) (P<0.01). Furthermore, relative hnRNPAB mRNA expression in SW480CSCs and HT29CSCs, compared with the parental cells, was 2.6- and 3.2-fold, respectively, as detected by RT-qPCR. (Fig. 3B). Moreover, the expression of hnRNPAB protein in SW480, SW480CSCs, HT29 and HT29CSCs were 0.74±0.04, 1.04±0.06, 0.68±0.03 and 0.98±0.07, respectively (Fig. 3C and D). These results indicate that compared with the parent cells, the expression level of miR-8063 in SW480CSCs and HT29CSCs was significantly decreased, while hnRNPAB expression was significantly increased (P<0.01).

miR-8063 expression is downregulated in human CRC tissues, which is associated with poor overall survival in patients with
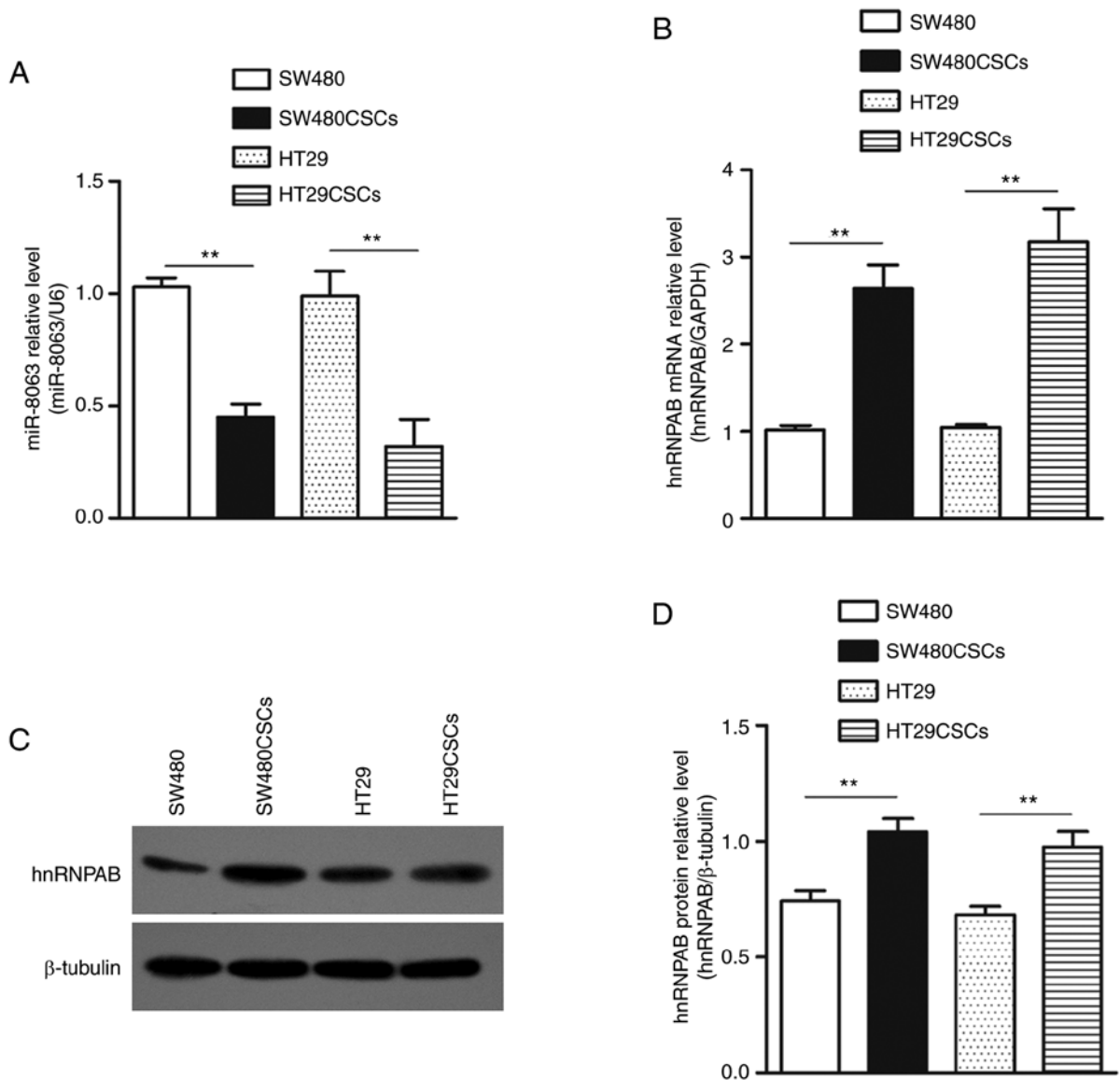
Figure 3. Expression of miR-8063 and hnRNPAB in colorectal cancer stem cells. (A) Expression of miR-8063 in SW480, SW480CSCs, HT29 and HT29CSCs was detected using RT-qPCR. (B) hnRNPAB mRNA relative expression in HT29CSCs and SW480CSCs were detected using RT-qPCR, compared with the parent cells. (C and D) Western blotting was used to detect the relative expression of hnRNPAB protein in SW480CSCs and HT29CSCs, compared with the parent cells. **P<0.01. miR, microRNA; hnRNPAB, heterogeneous nuclear ribonucleoprotein AB; CSC, cancer stem cells; RT-q, reverse transcription-quantitative.

CRC. The patient population comprised 65 men and 53 women (mean age, 58 years; age range, 30-82 years). Compared with the adjacent tissues, miR-8063 expression in CRC tissues was significantly downregulated (Fig. 4A; P<0.001). Next, the expression levels were classified as low and high according to the median value (0.62), and association between miR-8063 expression and patient clinicopathological characteristics was determined. As shown in Table I, low miR-8063 expression was significantly associated with advanced TNM stage (P=0.004), tumor infiltration (P=0.008), vascular invasion (P=0.010) and lymph node metastasis (P=0.020). No association was found between miR-8063 expression and age, sex, differentiation and tumor site. These data indicated that low expression of miR-8063 was closely associated with the malignant behaviors of CRC. The relationship between miR-8063 expression and the overall survival rate of patients was estimated using the Kaplan-Meier method; the overall survival rate of CRC patients with high miR-8063 expression was lower than those with low miR-8063 expression, suggesting an association between high expression and poorer prognosis (Fig. 4B; P=0.023).

hnRNPAB is a direct target gene of miR-8063. To verify whether there is a direct relationship between miR-8063 and hnRNPAB, bioinformatics software (TargetScan Human) was used to predict common binding sites between the two molecules. The results showed that the hnRNPAB gene possesses a potential miR-8063 binding sequence in its 3'UTR region (Fig. 5A). Furthermore, the dual-luciferase reporter assay revealed that compared with the other groups, the relative RLU value of the pmirGLO/hnRNPAB-3'UTR+miR-8063 mimics group was significantly lower (P<0.01), confirming that hnRNPAB is the direct target gene of miR-8063 (Fig. 5B and C) (P<0.01).
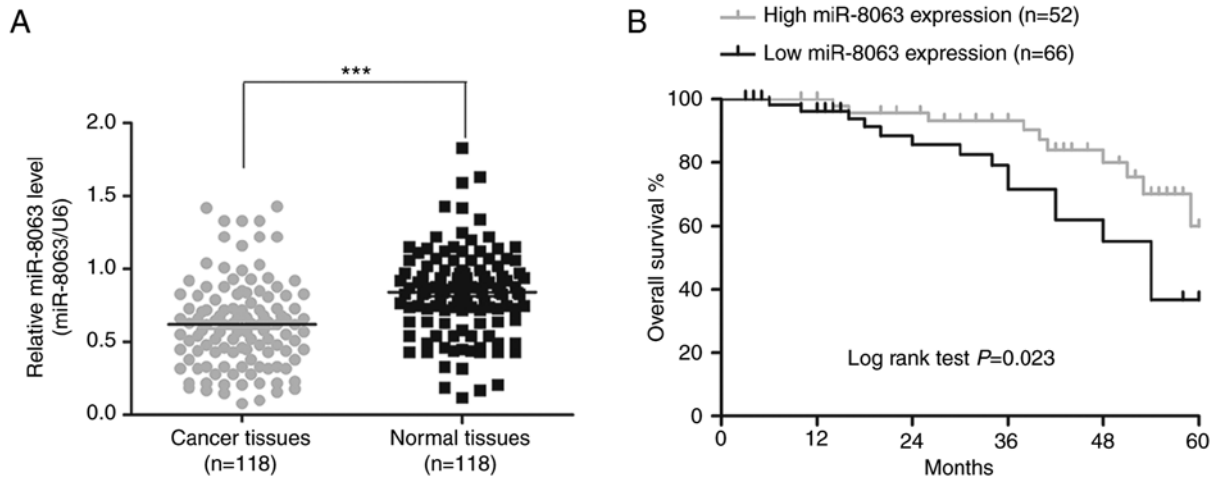
Figure 4. Expression of miR-8063 in CRC and its association with patient prognosis. (A) Expression of miR-8063 in human CRC tissues and paired adjacent normal tissues, ***P<0.001. (B) Kaplan-Meier curve of overall survival rate of patients with CRC. Compared with those with high expression, patients with low miR-8063 expression exhibited a worse prognosis. miR, microRNA; CRC, colorectal cancer.
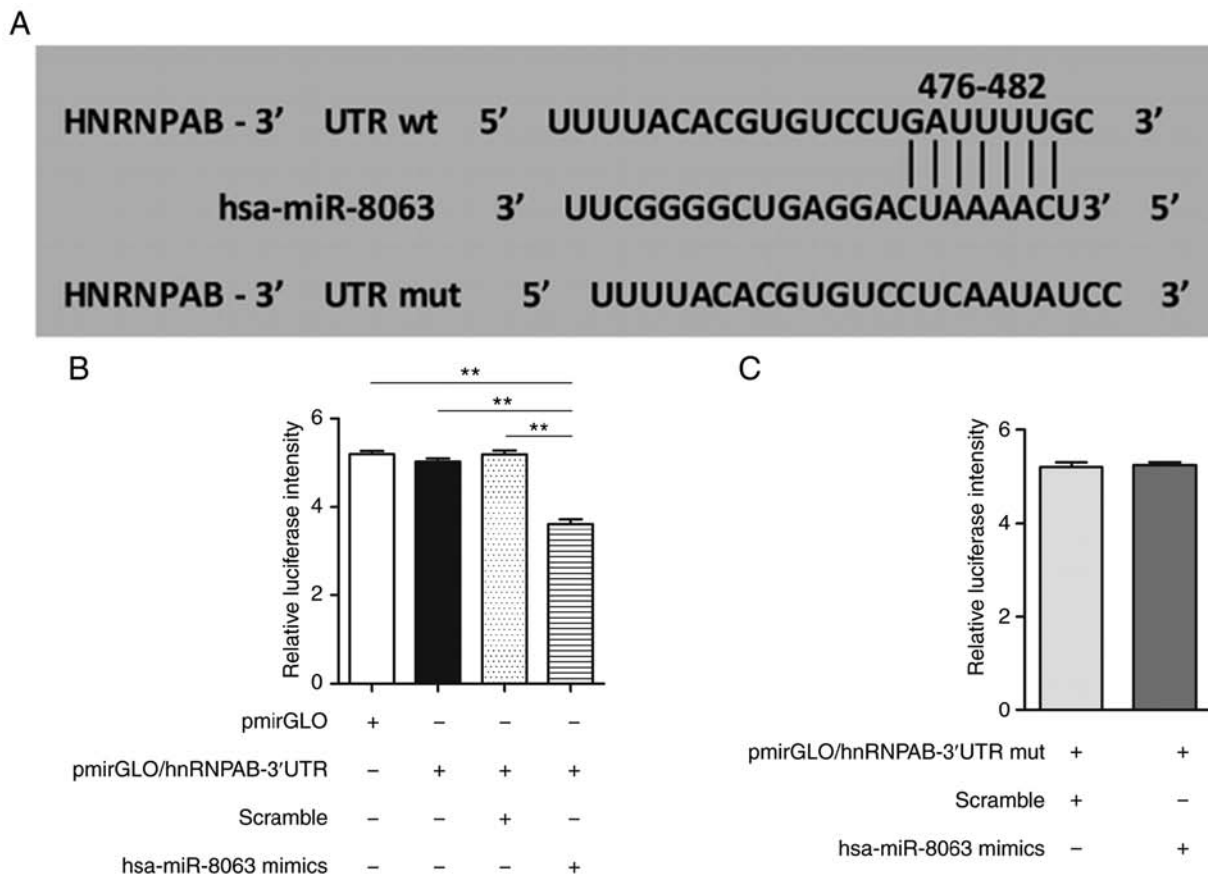

Figure 5. hnRNPAB is a direct target gene of miR-8063. (A) Predicted binding sites of miR-8063 in the 3'UTR of hnRNPAB were detected using the TargetScan Human online analysis tool. (B) Wild-type hnRNPAB 3'UTR fluorescence reporter assay. (C) Mutant hnRNPAB 3'UTR fluorescence reporter assay. **P<0.01. hnRNPAB, heterogeneous nuclear ribonucleoprotein AB; miR, microRNA; UTR, untranslated region.

Overexpression of hnRNPAB promotes the acquisition of stemness in SW480 and HT29 cells. To investigate the effect of hnRNPAB on the stemness of CRC cells, a lentiviral vector overexpressing hnRNPAB (hnRNPAB-GFP-PURO) and the corresponding NC (NC-GFP-PURO) were transfected into SW480 and HT29 cells, and the experimental groups (SW480-hnRNPAB and HT29-hnRNPAB) and

the NC group (SW480-NC and HT29-NC) were established. First, overexpression efficiency was tested. The hnRNPAB mRNA expression in the SW480-hnRNPAB and HT29-hnRNPAB groups was 3.5-fold and 3.3-fold, respectively, compared with that of the NC groups (Fig. 6A). The expression of hnRNPAB protein also showed a similar trend (Fig. 6B and C) (P<0.01). These results indicated
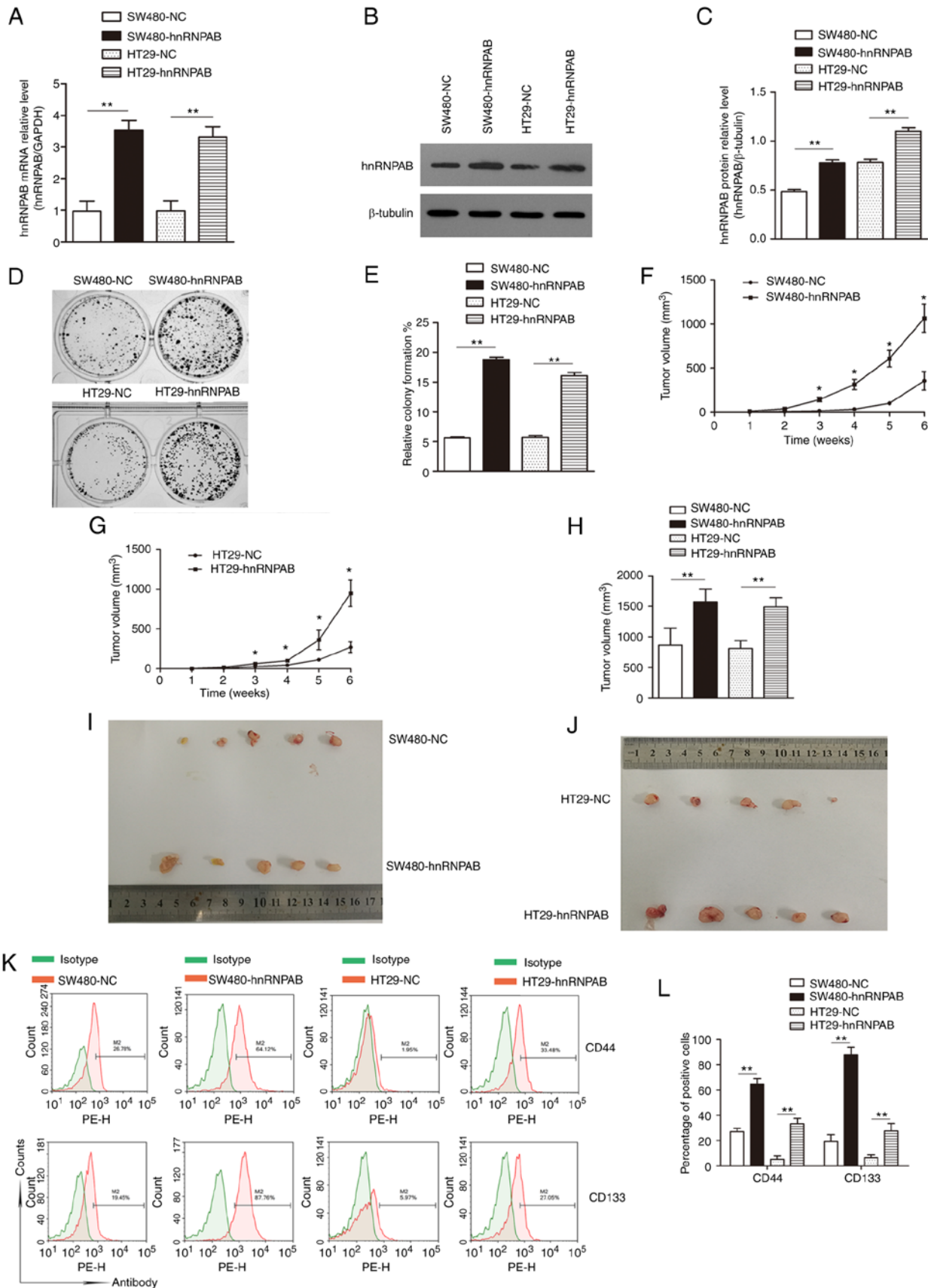
Figure 6. Overexpression of hnRNPAB promotes the acquisition of stemness in SW480 and HT29 cells. (A) Relative mRNA levels of hnRNPAB in the SW480-hnRNPAB and HT29-hnRNPAB groups detected by reverse transcription-quantitative PCR. (B and C) Western blotting was used to detect the protein levels of hnRNPAB in the SW480-hnRNPAB and HT29-hnRNPAB groups, compared with the NC groups. (D and E) Colony-formation rate of SW480-hnRNPAB and HT29-hnRNPAB groups, compared with those of the NC groups. (F and G) Tumor growth curve. (H) Tumor volume of SW480-hnRNPAB and HT29-hnRNPAB groups was significantly greater than that of the NC group. (I and J) Comparison of tumor volume *in vitro* between the experimental groups and the NC groups. (K and L) Percentage of CD133^{+} and CD44^{+} cells in SW480-NC, SW480-hnRNPAB, HT29-NC and HT29-hnRNPAB groups were detected using flow cytometry. $^*P<0.05$, $^{**}P<0.01$. hnRNPAB, heterogeneous nuclear ribonucleoprotein AB; NC, negative control.
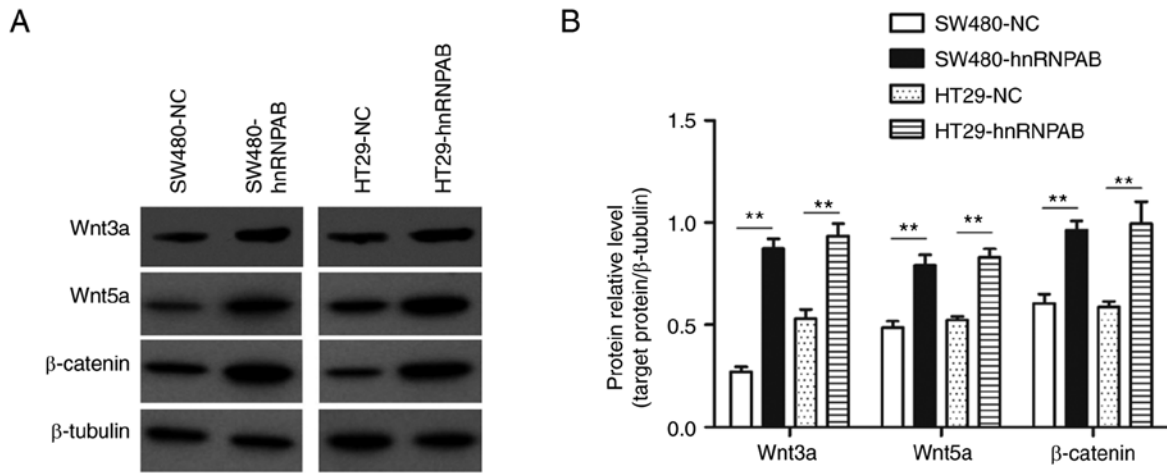
Figure 7. Overexpression of hnRNPAB activates the Wnt/β-catenin signaling pathway. (A) Protein expression of Wnt3a, Wnt5a and β-catenin in the SW480-NC, SW480hnRNPAB, HT29-NC and HT29-hnRNPAB groups was detected by western blotting. (B) Relative protein expression levels of Wnt3a, Wnt5a and β-catenin were calculated using β-tubulin as the internal reference. **P<0.01. hnRNPAB, heterogeneous nuclear ribonucleoprotein AB; NC, negative control.

that the hnRNPAB overexpression model was successfully constructed.

Furthermore, the colony formation rates of the SW480-hnRNPAB, SW480-NC, HT29-hnRNPAB and HT29-NC groups were 18.8±0.42, 5.6±0.21, 16.1±0.53 and 5.7±0.31%, respectively, indicating a significant increase in the colony-formation ability of SW480 and HT29 cells following hnRNPAB overexpression (Fig. 6D and E) (P<0.01).

The results of tumor formation in nude mice showed that all groups formed tumors, though the SW480-hnRNPAB and HT29-hnRNPAB groups exhibited increased tumor volumes compared with the NC groups (Fig. 6F and G). Similarly, the SW480-hnRNPAB and HT29-hnRNPAB groups possessed a significantly greater tumor volume than the NC-treated mice (Fig. 6H-J). These findings suggested that the tumorigenicity of CRC cells was significantly increased following hnRNPAB overexpression.

In addition, the proportions of CD44+ cells in the SW480-NC, SW480-hnRNPAB, HT29-NC and HT29-hnRNPAB groups were determined by flow cytometry, and were 27.05±2.57, 64.68±4.40, 5.08±2.72 and 33.27±5.27%, respectively. The corresponding proportions of CD133+ cells were 19.19±5.49, 87.88±6.18, 6.37±2.26 and 27.62±5.89% respectively (Fig. 6K and L) (P<0.01). These results suggested that the positive expression rates of CD44 and CD133 in the SW480-hnRNPAB and HT29-hnRNPAB groups were significantly greater than those of the corresponding NC groups.

Overexpression of hnRNPAB activates the Wnt/β-catenin signaling pathway. The relative protein expression levels of Wnt3a in the SW480-NC, SW480-hnRNPAB, HT29-NC and HT29-hnRNPAB groups were 0.27±0.03, 0.87±0.04, 0.52±0.04 and 0.91±0.03, respectively; and those of Wnt5a were 0.37±0.04, 0.92±0.05, 0.28±0.05 and 1.01±0.06, respectively. The corresponding protein expression levels of β-catenin in the four groups were 0.61±0.06, 0.96±0.06, 0.59±0.04 and 0.99±0.15, respectively. Thus, compared with the NC groups, the expression of Wnt/β-catenin pathway proteins in the experimental groups was significantly increased (Fig. 7A and B) (P<0.01).

Overexpression of miR-8063 inhibits self-renewal of SW480CSCs and HT29CSCs. SW480CSCs and HT29CSCs (obtained from SW480 and HT29 cells by suspension culture) were transfected with a lentiviral vector overexpressing miR-8063 and the corresponding NC. The experimental groups (SW480CSCs-miR-8063 and HT29CSCs-miR-8063) and NC groups (SW480CSCs-NC and HT29CSCs-NC) were established. Compared with the NC group, the SW480CSCs-miR-8063 and HT29CSCs-miR-8063 groups exhibited 2.7-fold and 3.3-fold relative expression of miR-8063, respectively, as detected by RT-qPCR (Fig. 8A; P<0.01).

The colony formation rates of the SW480CSCs-miR-8063, SW480CSCs-NC, HT29CSCs-miR-8063 and HT29CSCS-NC groups were 17.43±4.30, 42.59±3.48, 39.52±7.28, and 74.93±8.52%, respectively. Compared with those in the NC groups, the colony formation rates in the experimental groups were significantly decreased (Fig. 8B and C) (P<0.01). These results showed that following miR-8063 overexpression, the colony-formation ability of SW480CSCs and HT29CSCs was significantly decreased.

Following subcutaneous inoculation, the subcutaneous tumor growth of nude mice was observed weekly, and a growth curve was plotted (Fig. 8D and E). While all the groups formed tumors, the tumor volumes in the SW480CSCs-miR-8063 and HT29CSCs-miR-8063 groups were significantly lower than those of the corresponding NC-treated mice (Fig. 8F and G), suggesting that the tumorigenic ability of SW480CSCs and HT29CSCs in nude mice was significantly reduced by the overexpression of miR-8063.

The positive expression rates of CD44 in the SW480CSCs-miR-8063, SW480CSCs-NC, HT29CSCs-miR-8063 and HT29CSCs-NC groups were 3.35±1.87, 24.86±3.27, 6.42±1.3 and 35.06±2.40%, respectively. The corresponding positive expression rates of CD133 were 31.33±2.61, 87.91±4.99, 10.47.±2.52 and 33.07±3.86%, respectively (Fig. 8H and I) (P<0.01). These results indicate that the expression of CD44+ and CD133+ in the SW480CSCS-miR-8063 and the HT29CSCS-miR-8063 groups was significantly lower than that in the NC groups.
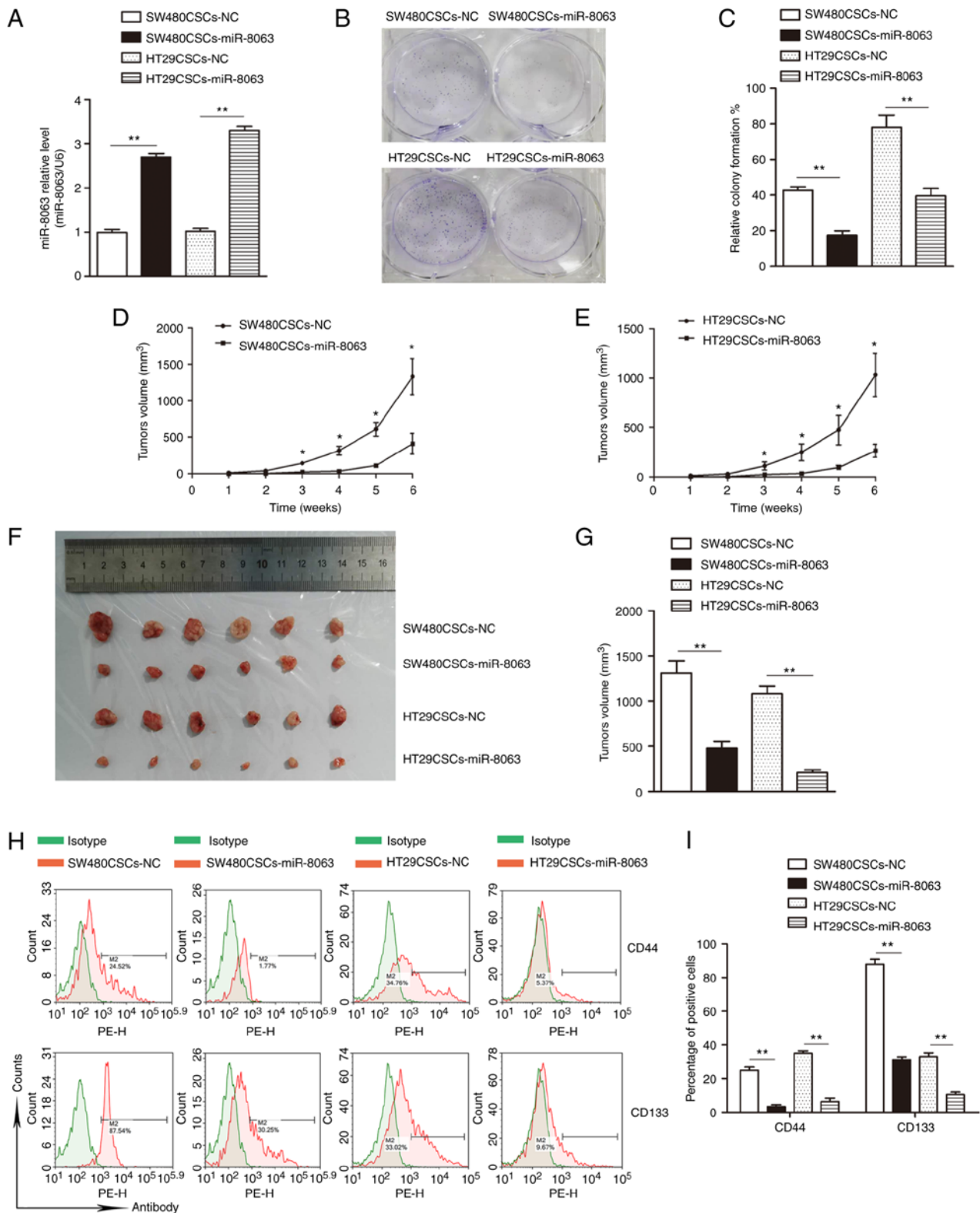
Figure 8. Overexpression of miR-8063 reduced the self-renewal of colorectal cancer stem cells. (A) Relative expression of miR-8063 detected using reverse transcription-quantity PCR, compared with those of the NC groups. (B and C) Colony-formation rate of SW480CSCs-miR-8063 and HT29CSCs-miR-8063 groups, compared with those of the NC groups. (D and E) Tumor growth curve. (F) Comparison of tumor volume *in vitro* between the experimental groups and the NC groups. (G) Histogram shows that the tumor volumes of SW480CSCs-miR-8063 and HT29CSCs-miR-8063 groups were significantly smaller than those of the NC groups. (H and I) Expression levels of CD44+ and CD133+ in SW480CSCs-NC, SW480CSCs-miR-8063, HT29CSCs-NC and HT29CSCs-miR-8063 groups were detected by flow cytometry. *P<0.05, **P<0.01. miR, microRNA; NC, negative control; CSC, cancer stem cells.

Overexpression of miR-8063 inhibits the expression of hnRNPAB, thus inhibiting the Wnt/β-catenin signaling pathway. The mRNA expression levels of hnRNPAB in the

SW480CSCS-NC, SW480CSCS-miR-8063, HT29CSCS-NC and HT29CSCS-miR-8063 groups were 1.03±0.11, 0.68±0.04, 0.96±0.05 and 0.53±0.02, respectively (Fig. 9A; P<0.01). The
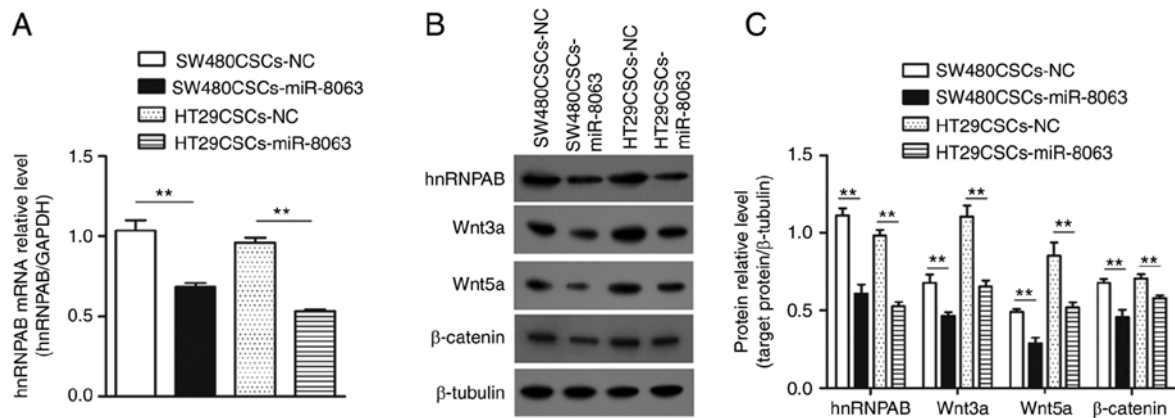
Figure 9. Expression of hnRNPAB, Wnt3a, Wnt5a and β-catenin after miR-8063 overexpression in SW480CSCs and HT29CSCs. (A) Relative hnRNPAB mRNA expression in SW480CSCS-miR-8063 and HT29CSCS-miR-8063 groups were detected using reverse transcription-quantitative PCR. (B and C) Relative protein expression of hnRNPAB, Wnt3a, Wnt5a and β-catenin in SW480CSCs-miR-8063 and HT29CSCs-miR-8063 groups was detected by western blotting using β-tubulin as the internal reference. **P<0.01. hnRNPAB, heterogeneous nuclear ribonucleoprotein AB; miR, microRNA; NC, negative control; CSC, cancer stem cells.

same trend was observed for protein expression of hnRNPAB (Fig. 9B and C; P<0.01). These results indicated that overexpression of miR-8063 inhibited the hnRNPAB expression.

Next, the relative protein expression of Wnt3a in the SW480CSCS-NC, SW480CSCS-miR-8063, HT29CSCS-NC and HT29CSCS-miR-8063 groups was 0.68±0.09, 0.47±0.04, 1.10±0.13 and 0.65±0.047, respectively. Concerning Wnt5a, the relative protein expression in the four groups was 0.49±0.03, 0.29±0.06, 0.85±0.15 and 0.52±0.06, respectively. The corresponding relative expression of the β-catenin protein was 0.68±0.04, 0.46±0.08, 0.71±0.05 and 0.58±0.03, respectively. Compared with the corresponding NC group, the expression levels of the three proteins in the SW480CSCs-miR-8063 and HT29CSCs-miR-8063 groups were significantly decreased (Fig. 9B and C; P<0.01). These results suggest that the overexpression of the miR-8063 gene inhibited the Wnt/β-catenin signaling pathway.

Silencing miR-8063 promotes the expression of hnRNPAB and activates the Wnt/β-catenin signaling pathway. miR-8063 was silenced in SW480 and HT29 cells using the lentiviral-mediated RNA interference (RNAi) technique, and experimental groups (SW480-sh-miR-8063 and HT29-sh-miR-8063) and NC groups (SW480-sh-NC and HT29-sh-NC) transfected with NC virus were established. Compared with the NC groups, the relative expression of miR-8063 in the experimental groups was significantly decreased (Fig. 10A; P<0.01). The results of RT-qPCR showed that compared with the NC group, the relative expression of hnRNPAB mRNA in the SW480-sh-miR-8063 and HT29-sh-miR-8063 groups was 2.9-fold and 5.7-fold, respectively (Fig. 10B; P<0.01). Similarly, the expression of hnRNPAB protein (detected by western blotting) was also significantly upregulated compared with that of the NC groups (Fig. 10C and D). These results indicated that hnRNPAB expression was upregulated following miR-8063 silencing. Next, we examined whether the upregulation of hnRNPAB expression induced by silencing miR-8063 was accompanied by the activation of the Wnt/β-catenin

signaling pathway. Compared with the NC groups, the relative expression levels of Wnt3a, Wnt5a and β-catenin in the SW480CSCs-miR-8063 and HT29CSCs-miR-8063 groups were significantly increased (Fig. 10C and D) (P<0.01). These findings suggest that miR-8063 silencing promoted the expression of hnRNPAB, resulting in the activation of the Wnt/β-catenin signaling pathway.

Discussion

According to the CSC theory, these cells are the root cause of cancer recurrence, metastasis and drug resistance. Therefore, direct targeting of CSCs is predicted to reverse chemotherapeutic resistance and prevent cancer recurrence and metastasis, thus potentially eradicating the associated cancers. Therefore, the regulatory mechanism and related therapeutic targets of CSCs are the focus of current cancer research (44). Due to the small proportion of CSCs in cancer tissue, the enrichment of these cells for further research is a challenge. The enrichment of CSCs using chemotherapeutics (45) and suspension culture (11) has been described in our previous study. In addition, various studies have indicated that CSCs can be enriched by flow cytometry (46) or magnetic activated cell sorting (47) for specific CSC markers.

Due to morphological similarities, it is difficult to distinguish CSCs from tumor cells; hence, the identification of CSCs is largely based on their self-renewal ability, tumorigenicity after transplantation into immunodeficient mice, and the expression level of specific cell surface markers (48,49). *In vivo* and *in vitro* experiments can be performed for CSC identification and characterization. For *in vivo* experiments, CSCs can form tumors when inoculated into immunodeficient mice, while general cancer cells cannot, or possess weak tumorigenic ability. By contrast, *in vitro* experiments encompass the use of soft agar colony formation to verify the self-renewal ability of CSCs; CSCs can form colonies on soft agar medium, but general cancer cells do not, or have reduced ability to form colonies. In addition, CSCs possess stemness, and the expression of specific cell surface markers
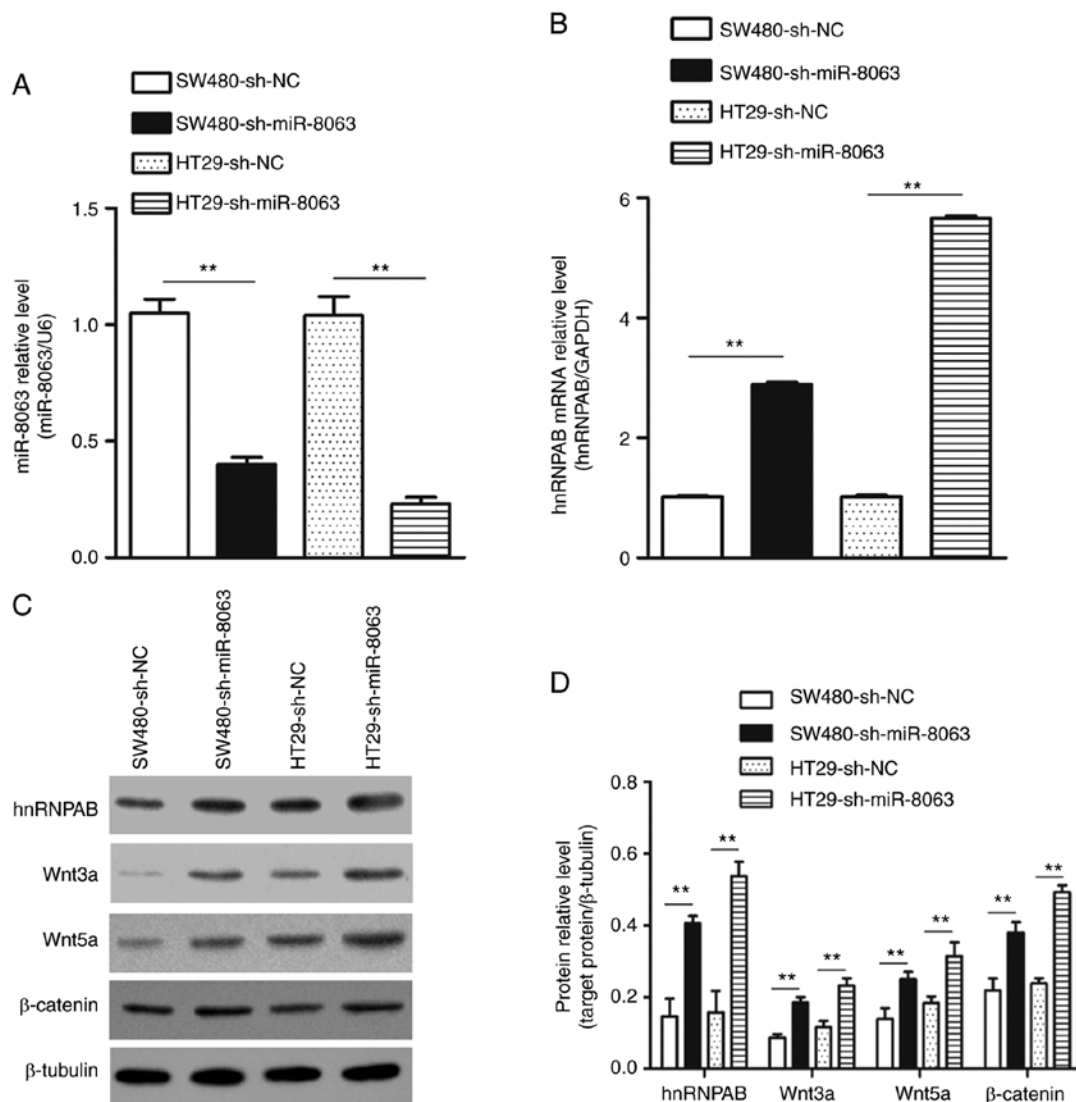
Figure 10. Expression of hnRNPAB, Wnt3a, Wnt5a and β-catenin after silencing miR-8063 in SW480 and HT29 cells. (A) Relative expression level of miR-8063 in SW480-sh-miR-8063 and HT29-sh-miR-8063 groups was detected using RT-qPCR, compared with those of the NC groups. (B) hnRNPAB mRNA expression in SW480-sh-miR-8063 and HT29-sh-miR-8063 groups was detected by RT-qPCR, compared with the NC groups. (C and D) Protein expression of hnRNPAB, Wnt3a, Wnt5a and β-catenin in SW480-sh-miR-8063 and HT29-sh-miR-8063 groups was detected by western blotting, compared with the NC groups. **P<0.01. hnRNPAB, heterogeneous nuclear ribonucleoprotein AB; miR, microRNA; NC, negative control; CSC, cancer stem cells; RT-q, reverse transcription-quantitative.

is significantly upregulated. Following in-depth research, CD44 and CD133 are recognized markers of colorectal cancer stem cells (50,51). Furthermore, the SW480-3D microspheres obtained by suspension culture of SW480 cells (in serum-free medium containing growth factors such as EGF and bFGF) were confirmed to exhibit CSC characteristics in our previous study (11). In the present study, a soft agar colony formation experiment, flow cytometric detection of CSC markers CD44 and CD133, and NOD/SCID mouse tumorigenesis studies were used to determine whether HT29-3D microspheres exhibited CSC characteristics. Compared with parental cells, HT29-3D microspheres exhibited significantly enhanced colony forma- tion ability (Fig. 2A and B), NOD/SCID mice had significantly enhanced tumorigenic ability (Fig. 2C and D), and CD44 and CD133 had significantly upregulated positive expression rates (Fig. 2E and F). The results also showed that HT29-3D micro- spheres exhibited CSC characteristics.

Next, the expression levels of miR-8063 and hnRNPAB in SW480CSCs and HT29CSCs were detected to verify our previous microarray screening results. Compared with the parent cells, the expression of miR-8063 in SW480CSCs and HT29CSCs was significantly decreased (Fig. 3A), while hnRNPAB expression was significantly upregulated (Fig. 3B-D). It was also confirmed that the expression trend of hnRNPAB and OCT4B1 in CRCSCs was consistent, while hnRNPAB and miR-8063 showed the opposite expression trend.

hnRNPAB is highly expressed in CRC and is closely associated with cancer stage and poor prognosis, as indicated in our previous study (21). To verify miR-8063 expression in CRC tissues, and its relationship with prognosis, the expres- sion level of miR-8063 was determined in CRC tissues by RT-qPCR. The results showed that compared with the adjacent tissues, miR-8063 expression in CRC tissues was significantly

downregulated (Fig. 4A), which was associated with advanced TNM stage, tumor infiltration, vascular invasion and lymph node metastasis (Table I). Furthermore, patients with low miR-8063 expression had a worse prognosis (Fig. 4B). These results indicate that miR-8063 may be a tumor suppressor gene that negatively regulates the progression of CRC.

Using bioinformatics software, the existence of binding sites between miR-8063 and hnRNPAB was predicted (Fig. 5A), and through dual-luciferase experiments, hnRNPAB was further confirmed as a downstream gene of miR-8063 (Fig. 5B and C). Then, SW480 and HT29 cells were infected with a lentiviral vector overexpressing hnRNPAB. Consequently, the changes in CSC characteristics were assessed by plate colony formation assays, nude mouse tumor formation assays and flow cytometry. Compared with the NC groups, the overexpression of hnRNPAB significantly increased colony formation ability (Fig. 6D and E), tumorigenic ability in nude mice (Fig. 6H-J), and the positive expression rates of CSC markers, CD44 and CD133 (Fig. 6K and L). These results suggest that overexpression of hnRNPAB promotes the acquisition of CSC characteristics in SW480 and HT29 cells. Moreover, the Wnt/β-catenin signaling pathway has been shown to be involved in cellular proliferation and differentiation, regulation of tissue homeostasis, and maintenance of the self-renewal of CSCs (30-33). The expression of the Wnt/β-catenin signaling pathway proteins can be regulated by hnRNPAB and its subtypes (28,29). Therefore, the expression levels of Wnt3a, Wnt5a and β-catenin protein, involved in the Wnt/β-catenin signaling pathway, were detected using western blotting, and the expression levels of the three proteins were significantly increased (Fig. 7A and B). This suggests that the overexpression of the hnRNPAB gene activates the Wnt/β-catenin signaling pathway. These results indicate that hnRNPAB overexpression promotes the acquisition of stemness in SW480 and HT29 cells by activating the Wnt/β-catenin signaling pathway.

Subsequently, the effect of miR-8063 on the function of CRCSCs was further investigated by overexpressing miR-8063 in SW480CSCs and HT29CSCs. Following miR-8063 overexpression, the cell colony formation ability was significantly weaker than that of the control cells (Fig. 8B and C), and tumorigenicity in nude mice was significantly reduced (Fig. 8F and G). In addition, the positive expression rates of CD44 and CD133 were significantly downregulated (Fig. 8H and I). These results indicate that miR-8063 is important in regulating the self-renewal of CRCSCs.

To investigate the molecular mechanism underlying the regulation of CRCSCs using miR-8063, the expression level of hnRNPAB, which has a direct binding site for miR-8063, was detected. The results showed that overexpression of miR-8063 significantly inhibited hnRNPAB expression (Fig. 9A and B). Moreover, western blot analysis revealed that the expression levels of key proteins in the Wnt/β-catenin signaling pathway (Wnt3a, Wnt5a and β-catenin) decreased with the downregulation of hnRNPAB (Fig. 9B and C). The expression level of hnRNPAB in SW480 and HT29 cells was detected after miR-8063 silencing using a lentiviral-mediated RNAi technique. The mRNA and protein expression of hnRNPAB were significantly upregulated after miR-8063 silencing (Fig. 10B-D). The expression of Wnt3a, Wnt5a and β-catenin were also increased following the upregulation of hnRNPAB (Fig. 10C and D). These

results indicated that hnRNPAB expression was upregulated, and that the Wnt/β-catenin signaling pathway was activated, after silencing the miR-8063 gene.

In conclusion, the present study confirmed that as a tumor suppressor, miR-8063 is involved in regulating the self-renewal of CRCSCs, and its molecular mechanism is through the loss of miR-8063 expression, which weakens its inhibition on hnRNPAB; this leads to the activation of the Wnt/β-catenin signaling pathway to promote the self-renewal of CRCSCs. These results provide new insights into the molecular targeted therapy of CRC, and highlight miR-8063 and hnRNPAB as potential therapeutic targets.

Availability of data and materials

The datasets used and/or analyzed during the current study are available from the corresponding author on reasonable request.

Authors' contributions

ZQC, TY, HJ and KMW conceived and designed the study. ZQC, TY, HJ and LW performed the experiments and data analysis. TY and HJ performed the cytological experiments. YYY, RMF, SQL, TZ, ZYW and KMW participated in the discussion and interpretation of data. TY and KMW confirm the authenticity of all the raw data. TY wrote the paper. KMW supervised all experimental work. All authors have read and approved the final manuscript.

Ethis approval and consent to participate

Human primary CRC tissues were obtained from patients admitted to the Department of Gastrointestinal Surgery, Affiliated Hospital of Zunyi Medical University. The present study was reviewed and approved by the Ethics Review Committee of the Affiliated Hospital of Zunyi Medical University (approval no. [2015] 1-040) and was conducted according to the recognized ethical guidelines (Declaration of Helsinki, CIOMS). All patients included in the study provided written informed consent. All animal experiments complied with Animal Research: Reporting *In Vivo* Experiment Guidelines, and were approved by the Animal Experiment Ethics Committee of Zunyi Medical University (approval no. [2015] 2-030).

Patient consent for publication

Not applicable.

Competing interests

The authors declare that they have no competing interests.

References

1. Sung H, Ferlay J, Siegel RL, Laversanne M, Soerjomataram I, Jemal A and Bray F: Global cancer statistics 2020: GLOBOCAN estimates of incidence and mortality worldwide for 36 cancers in 185 countries. CA Cancer J Clin 71: 209-249, 2021.
2. Miller KD, Nogueira L, Mariotto AB, Rowland JH, Yabroff KR, Alfano CM, Jemal A, Kramer JL and Siegel RL: Cancer treatment and survivorship statistics, 2019. CA Cancer J Clin 69: 363-385, 2019.
3. Das PK, Pillai S, Rakib MA, Khanam JA, Gopalan V, Lam AKY and Islam F: Plasticity of cancer stem cell: Origin and role in disease progression and therapy resistance. Stem Cell Rev Rep 16: 397-412, 2020.
4. Kuşoğlu A and Avcı ÇB: Cancer stem cells: A brief review of the current status. Gene 681: 80-85, 2019.
5. Yadav AK and Desai NS: Cancer stem cells: Acquisition, characteristics, therapeutic implications, targeting strategies and future prospects. Stem Cell Rev Rep 15: 331-355, 2019.
6. Bakhshinyan D, Adile AA, Qazi MA, Singh M, Kameda-Smith MM, Yelle N, Chokshi C, Venugopal C and Singh SK: Introduction to cancer stem cells: Past, present, and future. Methods Mol Biol 1692: 1-16, 2018.
7. Battle E and Clevers H: Cancer stem cells revisited. Nat Med 23: 1124-1134, 2017.
8. Lee SH, Reed-Newman T, Anant S and Ramasamy TS: Regulatory role of quiescence in the biological function of cancer stem cells. Stem Cell Rev Rep 16: 1185-1207, 2020.
9. Najafi M, Mortezaee K and Majidpoor J: Cancer stem cell (CSC) resistance drivers. Life Sci 234: 116781, 2019.
10. Steinbichler TB, Dudas J, Skvortsov S, Ganswindt U, Riechelmann H and Skvortsova II: Therapy resistance mediated by cancer stem cells. Semin Cancer Biol 53: 156-167, 2018.
11. Zhou JM, Hu SQ, Jiang H, Chen YL, Feng JH, Chen ZQ and Wen KM: OCT4B1 promoted EMT and regulated the self-renewal of CSCs in CRC: Effects associated with the balance of miR-8064/PLK1. Mol Ther Oncolytics 15: 7-20, 2019.
12. Geuens T, Bouhy D and Timmerman V: The hnRNP family: Insights into their role in health and disease. Hum Genet 135: 851-867, 2016.
13. Wang TH, Chen CC, Hsiao YC, Lin YH, Pi WC, Huang PR, Wang TCV and Chen CY: Heterogeneous nuclear ribonucleoproteins A1 and A2 function in telomerase-dependent maintenance of telomeres. Cancers (Basel) 11: 334, 2019.
14. Weighardt F, Biamonti G and Riva S: The roles of heterogeneous nuclear ribonucleoproteins (hnRNP) in RNA metabolism. Bioessays 18: 747-756, 1996.
15. Han SP, Tang YH and Smith R: Functional diversity of the hnRNPs: Past, present and perspectives. Biochem J 430: 379-392, 2010.
16. Xuan Y, Wang J, Ban L, Lu JJ, Yi C, Li Z, Yu W, Li M, Xu T, Yang W, et al: hnRNPA2/B1 activates cyclooxygenase-2 and promotes tumor growth in human lung cancers. Mol Oncol 10: 610-624, 2016.
17. Hu Y, Sun Z, Deng J, Hu B, Yan W, Wei H and Jiang J: Splicing factor hnRNPA2B1 contributes to tumorigenic potential of breast cancer cells through STAT3 and ERK1/2 signaling pathway. Tumour Biol 39: 1010428317694318, 2017.
18. Shi X, Ran L, Liu Y, Zhong SH, Zhou PP, Liao MX and Fang W: Knockdown of hnRNP A2/B1 inhibits cell proliferation, invasion and cell cycle triggering apoptosis in cervical cancer via PI3K/AKT signaling pathway. Oncol Rep 39: 939-950, 2018.
19. Ma Y, Yang L and Li R: HnRNPA2/B1 is a novel prognostic biomarker for breast cancer patients. Genet Test Mol Biomarkers 24: 701-707, 2020.
20. Yin D, Kong C and Chen M: Effect of hnRNPA2/B1 on the proliferation and apoptosis of glioma U251 cells via the regulation of AKT and STAT3 pathways. Biosci Rep 40: BSR20190318, 2020.
21. Zhou JM, Jiang H, Yuan T, Zhou GX, Li XB and Wen KM: High hnRNP AB expression is associated with poor prognosis in patients with colorectal cancer. Oncol Lett 18: 6459-6468, 2019.
22. Zhou ZJ, Dai Z, Zhou SL, Hu ZQ, Chen Q, Zhao YM, Shi YH, Gao Q, Wu WZ, Qiu SJ, et al: HNRNPAB induces epithelial-mesenchymal transition and promotes metastasis of hepatocellular carcinoma by transcriptionally activating SNAIL. Cancer Res 74: 2750-2762, 2014.
23. Tauler J, Zudaire E, Liu H, Shih J and Mulshine JL: hnRNP A2/B1 modulates epithelial-mesenchymal transition in lung cancer cell lines. Cancer Res 70: 7137-7147, 2010.
24. Dai S, Zhang J, Huang S, Lou B, Fang B, Ye T, Huang X, Chen B and Zhou M: HNRNPA2B1 regulates the epithelial-mesenchymal transition in pancreatic cancer cells through the ERK/snail signalling pathway. Cancer Cell Int 17: 12, 2017.
25. Shibue T and Weinberg RA: EMT, CSCs, and drug resistance: The mechanistic link and clinical implications. Nat Rev Clin Oncol 14: 611-629, 2017.
26. Cai Z, Cao Y, Luo Y, Hu H and Ling H: Signalling mechanism(s) of epithelial-mesenchymal transition and cancer stem cells in tumour therapeutic resistance. Clin Chim Acta 483: 156-163, 2018.
27. Nishiyama M, Tsunedomi R, Yoshimura K, Hashimoto N, Matsukuma S, Ogihara H, Kanekiyo S, Iida M, Sakamoto K, Suzuki N, et al: Metastatic ability and the epithelial-mesenchymal transition in induced cancer stem-like hepatoma cells. Cancer Sci 109: 1101-1109, 2018.
28. Stockley J, Villasevil ME, Nixon C, Ahmad I, Leung HY and Rajan P: The RNA-binding protein hnRNPA2 regulates β-catenin protein expression and is overexpressed in prostate cancer. RNA Biol 11: 755-765, 2014.
29. Meng X, Cui J, Wang Y, Zhang X, Li D, Hai Y and Du H: Heterogeneous nuclear ribonucleoprotein A1 interacts with microRNA-34a to promote chondrogenic differentiation of mesenchymal stem cells. Am J Transl Res 9: 1774-1782, 2017.
30. Jiang S, Song C, Gu X, Wang M, Miao D, Lv J and Liu Y: Ubiquitin-specific peptidase 22 contributes to colorectal cancer stemness and chemoresistance via Wnt/β-catenin pathway. Cell Physiol Biochem 46: 1412-1422, 2018.
31. Cheng X, Xu X, Chen D, Zhao F and Wang W: Therapeutic potential of targeting the Wnt/β-catenin signaling pathway in colorectal cancer. Biomed Pharmacother 110: 473-481, 2019.
32. Martin-Orozco E, Sanchez-Fernandez A, Ortiz-Parra I and Ayala-San Nicolas M: WNT signaling in tumors: The way to evade drugs and immunity. Front Immunol 10: 2854, 2019.
33. Tang T, Guo C, Xia T, Zhang R, Zen K, Pan Y and Jin L: LncCCAT1 promotes breast cancer stem cell function through activating WNT/β-catenin signaling. Theranostics 9: 7384-7402, 2019.
34. Yao Q, Chen Y and Zhou X: The roles of microRNAs in epigenetic regulation. Curr Opin Chem Biol 51: 11-17, 2019.
35. Saliminejad K, Khorram Khorshid HR, Soleymani Fard S and Ghaffari SH: An overview of microRNAs: Biology, functions, therapeutics, and analysis methods. J Cell Physiol 234: 5451-5465, 2019.
36. Liu XM, Fu Q, Du Y, Yang YX and Cho WC: MicroRNA as regulators of cancer stem cells and chemoresistance in colorectal cancer. Curr Cancer Drug Targets 16: 738-754, 2016.
37. Guo JC, Yang YJ, Zhang JQ, Guo M, Xiang L, Yu SF, Ping H and Zhuo L: MicroRNA-448 inhibits stemness maintenance and self-renewal of hepatocellular carcinoma stem cells through the MAGEA6-mediated AMPK signaling pathway. J Cell Physiol 234: 23461-23474, 2019.
38. Jiang S, Miao D, Wang M, Lv J, Wang Y and Tong J: miR-30-5p suppresses cell chemoresistance and stemness in colorectal cancer through USP22/Wnt/β-catenin signaling axis. J Cell Mol Med 23: 630-640, 2019.
39. Mukohyama J, Isobe T, Hu Q, Hayashi T, Watanabe T, Maeda M, Yanagi H, Qian X, Yamashita K, Minami H, et al: miR-221 targets QKI to enhance the tumorigenic capacity of human colorectal cancer stem cells. Cancer Res 79: 5151-5158, 2019.
40. Cheng CW, Liao WL, Chen PM, Yu JC, Shiau HP, Hsieh YH, Lee HJ, Cheng YC, Wu PE and Shen CY: miR-139 modulates cancer stem cell function of human breast cancer through targeting CXCR4. Cancers (Basel) 13: 2582, 2021.
41. Ni H, Qin H, Sun C, Liu Y, Ruan G, Guo Q, Xi T, Xing Y and Zheng L: miR-375 reduces the stemness of gastric cancer cells through triggering ferroptosis. Stem Cell Res Ther 12: 325, 2021.
42. Livak KJ and Schmittgen TD: Analysis of relative gene expression data using real-time quantitative PCR and the 2(-Delta Delta C(T)) method. Methods 25: 402-408, 2001.

43. Naito S, von Eschenbach AC, Giavazzi R and Fidler IJ: Growth and metastasis of tumor cells isolated from a human renal cell carcinoma implanted into different organs of nude mice. Cancer Res 46: 4109-4115, 1986.
44. Gupta R, Bhatt LK, Johnston TP and Prabhavalkar KS: Colon cancer stem cells: Potential target for the treatment of colorectal cancer. Cancer Biol Ther 20: 1068-1082, 2019.
45. Wen K, Fu Z, Wu X, Feng J, Chen W and Qian J: Oct-4 is required for an antiapoptotic behavior of chemoresistant colorectal cancer cells enriched for cancer stem cells: Effects associated with STAT3/Survivin. Cancer Lett 333: 56-65, 2013.
46. Lin QY, Wang JQ, Wu LL, Zheng WE and Chen PR: miR-638 represses the stem cell characteristics of breast cancer cells by targeting E2F2. Breast Cancer 27: 147-158, 2020.
47. Erdogan S and Turkekul K: Neferine inhibits proliferation and migration of human prostate cancer stem cells through p38 MAPK/JNK activation. J Food Biochem 44: e13253, 2020.

48. Abbaszadegan MR, Bagheri V, Razavi MS, Momtazi AA, Sahebkar A and Gholamin M: Isolation, identification, and characterization of cancer stem cells: A review. J Cell Physiol 232: 2008-2018, 2017.
49. Bhutia SK, Naik PP, Praharaj PP, Panigrahi DP, Bhol CS, Mahapatra KK, Saha S and Patra S: Identification and characterization of stem cells in oral cancer. Methods Mol Biol 2002: 129-139, 2019.
50. Wang C, Xie J, Guo J, Manning HC, Gore JC and Guo N: Evaluation of CD44 and CD133 as cancer stem cell markers for colorectal cancer. Oncol Rep 28: 1301-1308, 2012.
51. Zahran AM, Rayan A, Fakhry H, Attia AM, Ashmawy AM, Soliman A, Elkady A and Hetta HF: Pretreatment detection of circulating and tissue CD133(+) CD44(+) cancer stem cells as a prognostic factor affecting the outcomes in Egyptian patients with colorectal cancer. Cancer Manag Res 11: 1237-1248, 2019.